Indian Journal of Science and Technology, Vol 9(48), DOI: 10.17485/ijst/2016/v9i48/104434, December 2016
ISSN (Print) : 0974-6846
ISSN (Online) : 0974-5645

Convective Heat Transfer and Stability of Oil –Based Nanofluid

Abdul hassan A Karamallah* and Azad Abdulhakeem Hussein

Department of Mechanical Engineering, University of Technology, 5 Broadway, Ultimo NSW 2007, Australia; dr_abdulhassank@yahoo.com, azad85eng@gmail.com

Abstract

Objectives: Design and building a dedicated device (test rig) for measuring the convective heat transfer coefficient for an oil – based nanofluid under a laminar flow regime and a uniform heat flux. Preparing a stable oil – based nanofluid. Measuring experiment the stability of oil – based on nanofluid. **Methods/Statistical Analysis:** The nanofluid was prepared via two steps method, with three different mixing processes. Lubricating oil was used as a host liquid with aluminum oxide (Al2O3) as nanoparticles, with two particle sizes of 80 nm and 30 nm and different concentrations of (0.2, 0.6, 1 and 2) %wt. In order to study the effect of nanofluids on heat transfer coefficient, a dedicated test rig designed and built consisting of horizontal copper pipe, oil gear pump, nanofluid tank, heater and heat exchanger as a major components of the rig in addition of the accessory components and measuring devices.The stability of the nanofluid measured experimentally with Zeta Potential Analyzer. **Findings:** The heat transfer coefficient increased with increasing of the particle loading and decrease the particle size, the maximum enhancement in heat transfer coefficient at 2% wt was (7.83% and 16.75%) for 80 nm and 30 nm particle sizes, respectively. The best stability was found to be with 30 nm particle size at lower particle loading of (0.2% wt) and this concentration was recommended to use due to the excellent stability, lower cost and almost unnoticeable increasing in pressure drop. The nanofluid stability decreases with increasing both the particle size and particle loading. **Application/Improvements:** The base fluid of the used nanofluids is lubricating oil of automobile engine and the study showed an enhancement in the heat transfer coefficient with small penalty in pressure drop especially for the samples of low concentration and smallest particle size.

Keywords: Convective Heat Transfer, Nanofluid, Nusselt Number, Oil-Based Nanofluid, Pressure Drop, Stability

1. Introduction

Lubrication is a substantial design parameter for any mechanical device[1]. From thermal – engineering point of view, oils is like many coolant liquids (e.g. water and ethylene glycol) has low thermal capabilities. Scientists and engineers tried to enhance the thermal performance of coolant liquids, and this could traced back to Maxwell – 1873, which used metallic particles to enhance the thermal conductivity of fluids, but at that time they used millimeter and micro-meter sized particles, which have many drawbacks like sedimentation, clogging micro-channels, high pressure drop and corrosion of components. All the above drawbacks now could be avoided with the new nanotechnology[2-4].

In[5] investigated experimentally the enhancement of heat transfer of poly-alpha-olefin oil with core and shell nanoparticles: carbon coated cobalt and carbon coated copper, using three different particle loading (0.5, 1 and 1.5) wt% and flow rate (10 to 100) ml/s with inlet temperature (50, 65 and 90) °C. The study showed that the carbon coated copper has the largest enhancement at a temperature of 65 °C and 1.0 wt% concentration and for the carbon coated cobalt the largest enhancement was at 90 °C and 1.5 wt% concentrations. The study showed also that at the same temperature, flow rate and concentration, the carbon coated copper has larger enhancement than carbon coated cobalt. In[6] studied the effect of particle size on heat transfer measurement using three different sizes of spherical copper nanoparticles (25, 40-60 and

*Author for correspondence

60-80) nm dispersed in PAO (poly-alpha-olefin) motor oil, heat transfer coefficient measured in a test section of copper tube with inner diameter of ¼ inch. The base fluid and nanofluid behaved like Newtonian fluid, also the heat transfer coefficient was increased with increasing Reynolds number, and also the best overall enhancement was with the smallest particle's size (25 nm). In[7] investigated experimentally the convective heat transfer of oil-based nanofluid flow inside an inclined copper tube with outer diameter of 12.7 mm, 0.9 mm wall thickness and 1200 mm length, under uniform heat flux condition and laminar flow regime fully developed, using CuO nanoparticles (50 nm) with particle loading (0.5, 1 and 2) wt.% , the study showed that the heat transfer coefficient increase with the increasing of Reynolds number inside horizontal and inclined tube, also at same Reynolds number, nanofluid flowing inside the inclined tube at 30 degree showed the most enhancement in heat transfer among other tube inclinations.

In the present work, the effect of particle size and particle loading on oil based nanofluid are investigated using two particle sizes of (30 and 80) nm and concentration of (0.2, 0.6, 1 and 2)% wt with different flow rates in hydro-dynamic fully developed laminar flow regime.

2. Materials

Mono – grade Rasheed motor oil (made in Iraq) was used as a base fluid, the oil has the following specifications:

SAE No.	40
Density g / cm3 @ 15 ° C	0.895
Viscosity (cst) @ 100 ° C	12.5 – 16.5
Viscosity index (min.)	95
Flash point ° C	230
Pour point ° C	–9

Al_2O_3 nanoparticles was suspended with two particle sizes of (30 and 80) nm in the oil, with the particle loading of (0.2, 0.6, 1 and 2) % wt.

3. Nanofluid Preparation

The nanofluid was prepare via two steps method, first step was obtaining the particles as a dry powder and second step was suspending the particles in the host liquid to create a stable suspension. The nanofluid is not a simple mixture, so special attention and techniques required during the preparation. The following steps were used to prepare the nanofluid: Direct mixing of the nanoparticles with the liquid. Using high mechanicals shear mixing to prevent the agglomeration of the nanoparticles. High mechanical shear mixing was generated by four blades propeller attached to a drilling machine, propeller diameter is 15 cm, the rod of the mixer located in the center of container with diameter of 21 cm, the electric impact drill from Celma – Poland have power of 710 W and 2600 rpm, the nanofluid was mixed with this device for about (20 – 30) min. Hand mixer: portable hand mixer from Studio - Germany used as a second step after the high mechanical shear mixing to ensure higher stability. Final step of mixing was to use close circulation inside the test rig by using only the gear pump, bypass line and nanofluid tank As shown in Figure 1, the circulation time is about (20 – 30) min.

4. Experimental Setup

The convective heat transfer test rig schematic diagram is shown in Figure 2. The apparatus consists of: major components, accessory components and measuring devices. The major components consists of: test section of copper

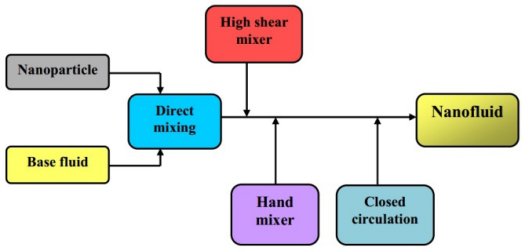

Figure 1. Block diagram of Nanofluid preparation.

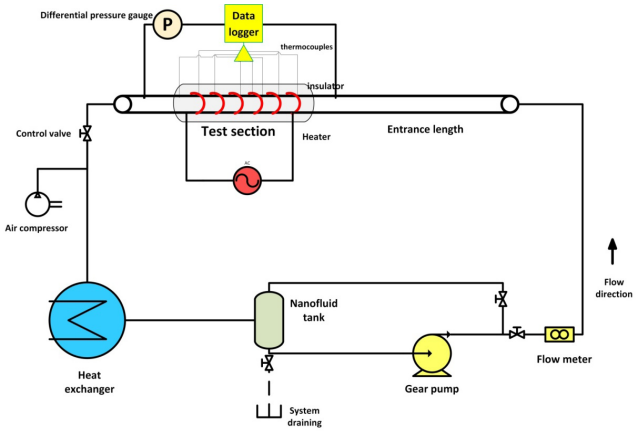

Figure 2. Experimental test rig schematic diagram.

horizontal tube with ⅜ inch outer diameter and 1 m length with 1.2 m prior the test section to ensure the fully – developed flow in the test section, Gear pump, an electrically insulated heater was wrapped around the test section to provide a constant heat flux, cylindrical Nanofluid tank, closed type spiral heat exchanger was used to remove heat from the system and ensure desirable inlet conditions in the test section. The accessory components consist of: Heat exchanger cooling cycle consist of (source tank, water pump and flow meter), control board, data logger, a contact voltage regulator, air compressor, control valves, insulators, piping and fittings. The measuring devices consist of: K – Type thermocouples screw style probe sensor (10 thermocouples, two of them penetrate the test section to measure the inlet and outlet temperature of the fluid and the other eight thermocouples are fixed on the tube surface), Oil flow sensor with digital readout, differential pressure gauge, volt meter and ampere meter.

5. Data Reduction

All the thermo – physical properties of oil – based nanofluids related to convective heat transfer coefficient were measured experimentally. The local heat transfer coefficient can be expressed by[8-12]:

$$h(x) = \frac{q''}{T_w(x) - T_f(x)} \quad (1)$$

where: x represents the axial distance from the inlet of the test section, q" is the heat flux, T_w is the wall temperature and T_f is the fluid temperature which calculate from the energy balance as[8,9,12]:

$$T_f = T_{in} + \frac{q'' \pi D X}{\dot{m}_{nf} Cp_{nf}} \quad (2)$$

Where: D is the pipe diameter $\dot{m}$ and C_p are the mass flow rate and specific heat of the nanofluid, respectively. T_{in} is the inlet temperature.

The average heat transfer coefficient is given by:

$$h_{avg.} = \frac{1}{L}\int_0^L h(X)dx \quad (3)$$

Nusselt number is calculated by:

$$Nu = \frac{hD}{K} \quad (4)$$

Where: K is the thermal conductivity of the liquid.

Friction factor is expressed by[8,9,12]:

$$f = \frac{\frac{\Delta P}{L} D}{\frac{\rho U^2}{2}} \quad (5)$$

where: ΔP is the pressure drop across the test section, L is the test section length, ρ is the density of the liquid and U is the velocity of the liquid.

6. Nanofluid Stability

Synthesis of stable nanofluid is a technical challenge, because the nanoparticles have a tendency to agglomerate and this agglomeration not only cause the sedimentation of the particles but also cause losing of the wanted enhancement in the thermal properties. The stability of the nanofluid measured experimentally of oil – based nanofluid for the 30 nm particle size and particle loading of (0.2, 0.6, 1 and 2) %wt. using Zeta Potential Analyzer device. Zeta potential is a physical property which is displayed by any particle in suspension[13-18].

7. Results and Discussion

7.1 Validation of the Experimental Test Rig

In order to validate the rig performance and the obtained data, the average Nusselt number of base fluid (oil) was compared with Hausen correlation, that applicable for uniform velocity inlets for Pr >> 1, thermal boundary layer develops in the presence of fully developed velocity profile (hydrodynamic fully developed flow) and laminar flow in circular tube.

$$Nu_D = 3.657 + \frac{0.668 \left(\frac{D}{L}\right) Re\, Pr}{1 + 0.04\left[\left(\frac{D}{L}\right) Re\, Pr\right]^{\frac{2}{3}}} \quad (6)$$

Figure 3 shows the comparison between experimental data of base liquid with Hausen correlation.

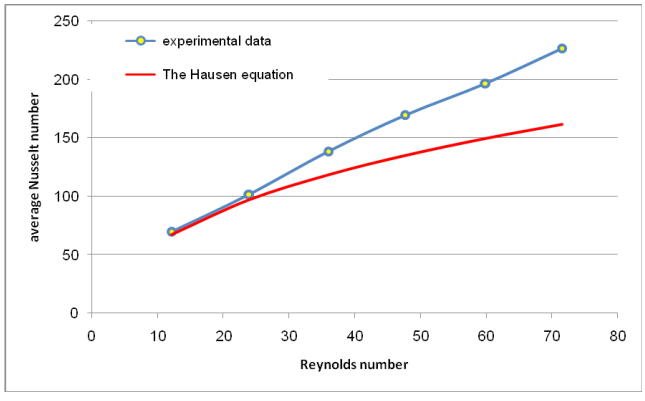

Figure 3. Comparison between experimental data of base liquid with Hausen correlation[19].

The friction factor of the base fluid (oil) also compared with Shah and London equation:

$$f * Re = \frac{3.44}{\sqrt{X}} + \frac{P_o + \frac{K}{4X} - 3.\frac{44}{\sqrt{X}}}{1 + 0.\frac{000212}{X^2}} \quad (7)$$

where: f is the friction factor, $X = \frac{L}{D}$, $K = 1.2 + (\frac{38}{Re})$ and P_o: Poiseuille number = 16 for circular shaped channels.

Figure 3 Comparison between experimental data of base liquid with Hausen correlation[19].

Figure 4 is the comparison between experimental data of base liquid with Shah and London correlation[19].

7.2 Effect on Tube Surface Temperature

The surface temperature decreased in the presence of the nanoparticles and that because of the enhancement in cooling. All nanofluids show lower surface temperature compare to the base fluid. As shown in Figures 5 to 7, the surface temperature distribution along the test section at different flow rates. The small fluctuation in experimental data is due to some localized heat (heat storage in some location or could be due to the effect of nanoparticles). The last point (last surface thermocouple) on the test section has a lower value than the previous point, due to cooling effect of the outlet temperature of the section.

Figure 5 the surface temperature distribution along the test section at 1 l/min.

Figure 6 the surface temperature distribution along the test section at 1.5 l/min.

Figure 7 the surface temperature distribution along the test section at 2.5 l/min.

7.3 Effect on Heat Transfer Coefficient and Nusselt Number

The enhancement in heat transfer coefficient is much more difficult to obtain than other properties such as

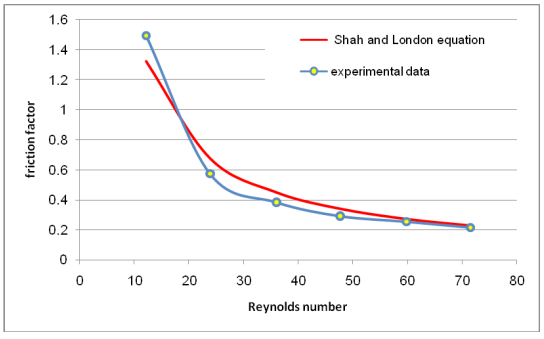

Figure 4. Comparison between experimental data of base liquid with Shah and London correlation [19].

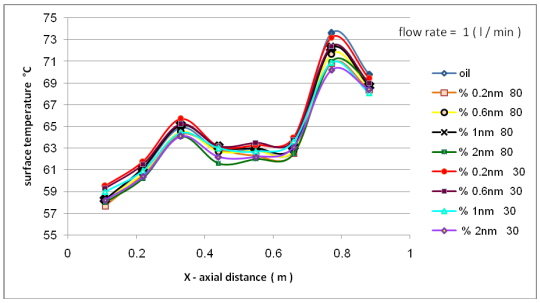

Figure 5. The surface temperature distribution along the test section at 1l/min.

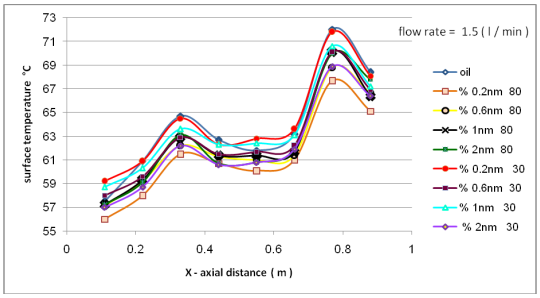

Figure 6. The surface temperature distribution along the test section at 1.5l/min.

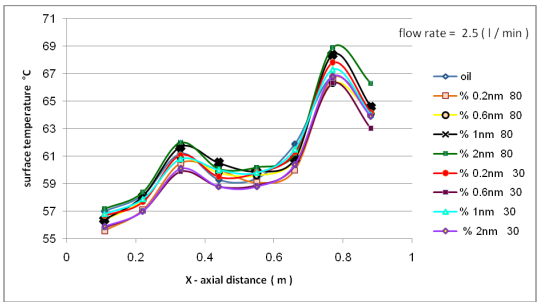

Figure 7. The surface temperature distribution along the test section at 2.5 l/min.

thermal conductivity, due to the effect of many factors. The high enhancement in some properties does not necessarily lead to high enhancement in heat transfer coefficient[20-23]. For 80 nm particle, the concentrations of (0.2 and 0.6) %wt did not show noticeable enhancement in heat transfer coefficient (less than 1.2%), the other concentrations (1 and 2) %wt show much higher values of enhancement of (4.97% and 7.83%) respectively. The 30 nm particle size showed more potential for heat transfer coefficient enhancement, for the concentrations (0.2, 0.6, 1 and 2) %wt the enhancement in heat transfer coefficient was (5.65%, 6.758%, 10.69% and 16.757%) respectively, as average enhancement for different flow rates. As shown in

Figure 8, the average heat transfer coefficient with different particle size and loading. The 30 nm sizes was much better than 80 nm, the higher enhancement in heat transfer coefficient for 30 nm size could be because of the smaller size lead to more chaotic motion (Brownian motion), as well as the high enhancement in thermal diffusivity and thermal conductivity. In term of the local heat transfer coefficient the higher value of heat transfer coefficient is in the entrance of the test section and decrease downstream along the test section, in spite of some fluctuation in experimental data and that could be due to localized heat (heat stored in a small amount in some positions of the tube). Figures 9 to 11 show the local heat transfer coefficient with different particle size and concentration with different flow rates.

Figure 8 average heat transfer coefficient with different particle size and loading.

Figure 9 local heat transfer coefficient with different particle size and concentration at 1 l/min.

Figure 10 local heat transfer coefficient with different particle size and concentration at 1.5 l/min.

Figure 11 local heat transfer coefficient with different particle size and concentration at 3 l/min.

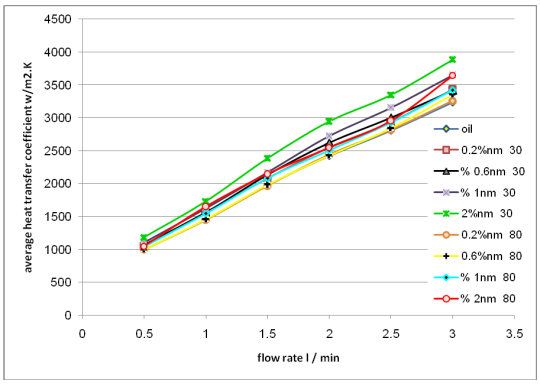

Figure 8. Average heat transfer coefficient with different particle size and loading.

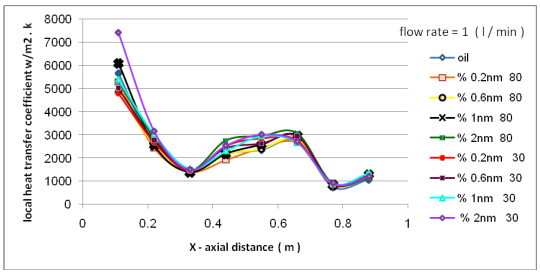

Figure 9. Local heat transfer coefficient with different particle size and concentration at 1 l/min.

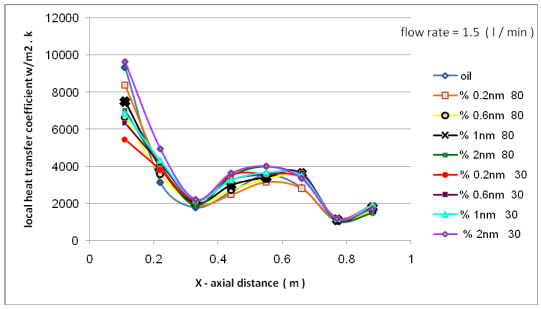

Figure 10. Local heat transfer coefficient with different particle size and concentration at 1.5 l/min.

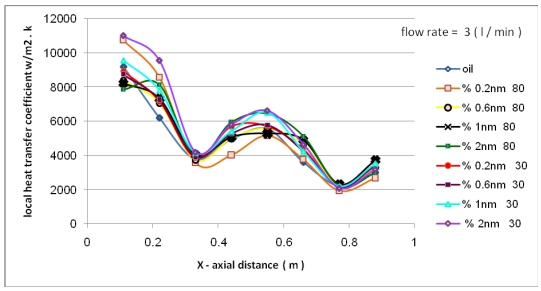

Figure 11. Local heat transfer coefficient with different particle size and concentration at 3 l/min.

Nusselt number decreases with increasing of the concentration and decreasing the particle size and that because the enhancement in thermal conductivity is much higher than the enhancement in heat transfer coefficient. Also, Nusselt number increase with the increasing of the flow rate. Figure 12 shows the average Nusselt number with different particle size and concentration.

Figure 12 average Nusselt number.

7.4 Effect on Friction Factor an Pressure Drop

Although one of the benefits of using the nanoparticles over other types of particles, is its small penalty in pressure drop, still the presence of the nanoparticles cause pressure drop. Pressure drop increased with increasing the particle concentration, particle size and increasing the flow rate. Maximum pressure drop was (13.04% and 20%) for 30 nm and 80 nm particle size respectively at 2% wt concentration and at highest used flow rate. Low concentration (0.2% wt) for both 30 nm and 80 nm did not show noticeable increase in pressure drop especially for 30 nm particle size and at low flow rates. As shown in Figure 13. Friction factor of the nanofluids show

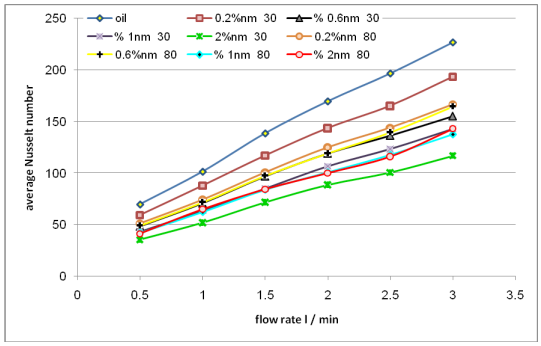

Figure 12. Average Nusselt number.

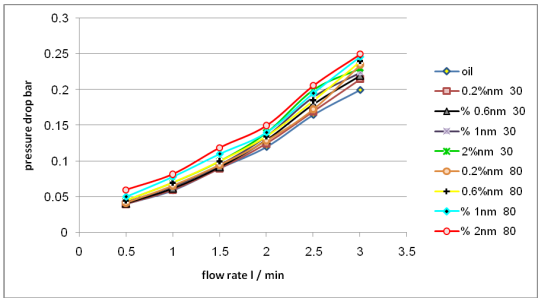

Figure 13. Pressure drop across the test section.

higher values than the base fluid, and it increased with the increasing the particle size and particle concentration and decreased with increasing the flow rate. The particle size 80 nm shows noticeable increase in friction factor especially for the concentrations of 1% wt and 2% wt and at low flow rate followed by 30 nm with concentration 2% wt. At higher flow rates the nanofluis did not show noticeable difference in friction factor compare with the base fluid, as shown in Figure (14).

Figure 13 pressure drop across the test section.

Figure 14 friction factors for different particle size and concentration.

7.5 Stability

Zeta Potential method is used for 30 nm particle size. The zeta potential values indicate that the suspensions with zeta potential above 30 mV (absolute value) are physically stable, suspensions with a potential above 60 mV show excellent stability. Suspensions below 20 mV gives limited stability and the suspensions undergo pronounced aggregation when the potential below 5 mV. For the 30 nm particle size, one concentration (0.2%wt) shows excellent stability, and (0.6% wt) shows good stability. The other concentrations (1% wt and 2% wt) give results below the physically stable line, as shown in Figure 15.

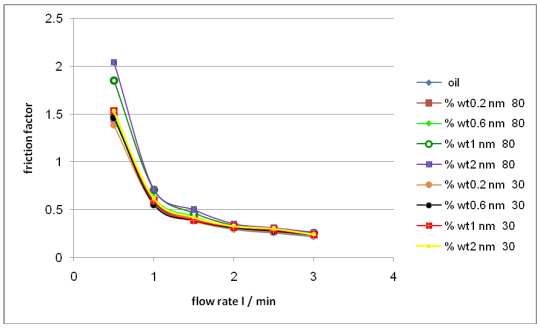

Figure 14. Friction factor for different particle size and concentration.

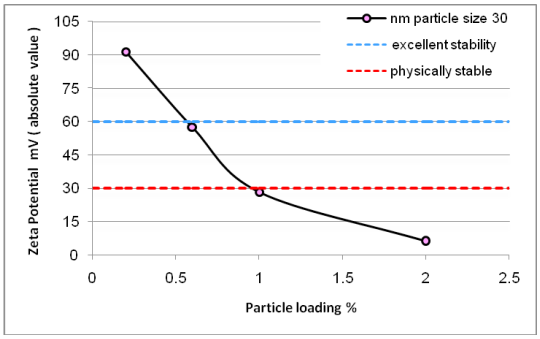

Figure 15. Zeta Potential for nanofluids with 30 nm particle size.

Figure 15 Zeta Potential for nanofluids with 30 nm particle size.

8. Conclusions

The heat transfer coefficient increased with increasing the concentration and decreasing the particle size. Maximum enhancement noticed at the highest concentration (2% wt) and found to be 7.83% and 16.75% for 80 nm and 30 nm particle size, respectively. Also, the higher heat transfer coefficient is obtained at the pipe entrance (test section entrance) and decreases along the axial distance of the pipe. The highest stability was found with lower concentration (0.2% wt) and smaller particle size (30 nm) and this recommended using due to the excellent stability, also due to the lower cost and almost unnoticeable increasing in pressure drop. The stability of the nanofluid decreases with increasing the particle size and particle loading.

9. Reference

1. Zhang Z, Zenyu Z, Simionesie S, Dorin D, Schaschke S, Carl C. Graphite and Hybrid Nanomaterials as Lubricant Additives, Lubricants. 2014; 2:44–65.

2. Dorinson A, Ludema KC. Mechanics and Chemistry in Lubrication. Elsevier: Amsterdam, The Netherlands, 1985.
3. Choi SU. Nanofluid Technology - Current Status and Future Research. Argonne, IL 60439, 1998.
4. Bianco V, Manca O, Nardini S, Vafai K. Heat Transfer Enhancement with Nanofluids. Taylor and Francis Group, LLC. 2015.
5. Milligan CA. An Investigation of Heat Transfer Enhancement in Nanofluids Containing Core and shell Nanoparticles. University of Louisville, 2014.
6. Liu K. Heat Transfer Measurement in oil – Based Nanofluid. University of Louisville, 2011.
7. Pirhayati M, Akhavan-Behabadi MA, Khayat M. Convective Heat Transfer of Oil Based Nanofluid Flow Inside a Circular Tube, International Journal of Engineering. IJE Transactions B : Applications. 2014 Feb; 27(2):341–48.
8. Al-Saady NS. Investigation of Heat Transfer Enhancement with Nanofluid and Twisted Tape Inserts in a Circular Tube. University of Technology, Baghdad, Iraq. 2014.
9. Sultan KF. An Investigation into Heat Transfer and Flow of Nanofluids in Circular Tube. University of Technology, Baghdad, Iraq. 2012.
10. Holman JP. Heat Transfer. McGraw – Hill Companies, Inc., Tenth Edition. 2010.
11. Holman JP. Experimental Methods for Engineers. McGraw – Hill Companies, Inc., Eighth Edition, 2012.
12. Asker AH. The Effect of Magnetic Field with Nanofluid on Heat Transfer in a Horizontal Pipe. University of Technology, Baghdad, Iraq. 2016.
13. Francisco e la Cruz E, Zheng Y, Torres E, Li W, Song W, Burugapalli K. Zeta Potential of Modified Multi-Walled Carbon Nanotubes in Presence of Poly (Vinyl Alcohol) Hydrogel, International Journal of Electrochemical Science. 2012; 7:3577–90.
14. Colloidal Dynamics, Electroacoustics Tutorial, The Zeta Potential. 1999.
15. Xu Y. Tutorial: Capillary Electrophoresis. Cleveland State University, Springer – verlay New York, Inc.1996.
16. Zeta Potential: An Introduction in 30 minute, Zetasizernano Series Technical Note, Malvern Instrument.
17. Zeta Potential Analysis of Nanoparticles, Nano Composix. September 2012; 11.
18. Júnior JA, Baldo JB. The Behavior of Zeta Potential of Silica Suspensions, New Journal of Glass and Ceramics. 2014; 4:29–37.
19. Thome JR. Engineering Data Book III. Faculty of Engineering Science and Technology, Swiss Federal Institute of Technology Lousanne (EPFL) CH – 1015 Lousanne, Switzerland, 2010, Wolverine Tube, Inc.
20. Sharma, Pandey KM. Numerical Investigation of Heat Transfer Characteristics in Triangular Channel in Light Water Nuclear Reactor by using CuO-Water based Nanofluids, Indian Journal of Science and Technology. 2016 Apr; 9(16):1–6.
21. Singh RN, Rajat P, Lav I, Pandey PK. Experimental Studies of Nanofluid TiO2/CuO in a Heat Exchanger (Double Pipe), Indian Journal of Science and Technology. 2016 Aug; 9(31):1–6.
22. Bakar NNA, Bachok N, Arifin N. Boundary Layer Flow and Heat Transfer in Nanofluid over a Stretching Sheet using Buongiorno Model and Thermophysical Properties of Nanoliquids, Indian Journal of Science and Technology. 2016 Aug; 9(31):1–9.
23. Kajla S, Sehgal SS. Computational Analysis on the Effects of CuO-Water based Nanofluids on the Performance of Flat Plate Solar Collector, Indian Journal of Science and Technology. 2016 Sep; 9(36):1–10.